Dispersion in Core–Annular Flow with a Solid Annulus

Marissa S. Fallon and Anuj Chauhan
Dept. of Chemical Engineering, University of Florida, Gainesville, FL 32611

DOI 10.1002/aic.10506
Published online June 20, 2005 in Wiley InterScience (www.interscience.wiley.com).

The Taylor dispersion of a solute is studied in a core–annular geometry. The fluid flows only through the core, but the solute can diffuse into the solid annulus. The long time limit of the dispersion coefficient D is derived by a regular expansion in the aspect ratio for two different scalings of the Biot number (Bi), which is the dimensionless interfacial mass-transfer resistance. The results for the case of O(1) Bi match those obtained by Aris and a number of other researchers. In the case of O(ε) Bi, where ε is the aspect ratio, the average mass-transfer equations for the core and the annulus are coupled and do not simplify to a simple convection–dispersion form. The average mass-transfer equations are derived for two velocity profiles: Poiseuille flow and plug flow. The dispersion coefficient for the limiting case when both the core and the annulus are radially well mixed at all times is also determined for the case of O(1) Bi. For O(1) Bi, the dispersion of the solute arises as a result of molecular diffusion, interfacial mass-transfer resistance, and convective flow, and the contribution from interfacial mass-transfer resistance is independent of the velocity profile. This dispersion coefficient reduces to the classical result of fluid flow through a tube in the limit of vanishing annulus thickness and also for the case when the solute has zero solubility in the solid. The core–annular geometry mimics the Krogh cylinder, which is a model used for analyzing mass transfer from capillaries into surrounding tissue. The model predictions for the dispersion coefficients in different tissues agree reasonably with the experimentally reported values, and the agreement is the best for muscles, where the Krogh cylinder model is expected to most closely resemble the actual physiology.* © 2005 American Institute of Chemical Engineers *AIChE J,* 51: 2415–2427, 2005

Keywords: Taylor dispersion, core–annular flow, transport in capillaries and tissues, mass transfer, Poiseuille flow, plug flow, Krogh cylinder

Introduction

The transport of solutes in geometries with large aspect ratios can usually be described in terms of an effective dispersion coefficient, frequently referred to as the Taylor dispersion coefficient, which quantifies the spread of a pulse of solute in the axial direction. Aris first modeled the problem of dispersion in a tube for a Newtonian fluid and obtained the classical result that the dispersion coefficient, D^*, is given by $D + (\langle u \rangle^2 R^2)/48D$,[1] where D, $\langle u \rangle$, and R are the molecular diffusivity, the mean fluid velocity, and the tube radius, respectively. Since then, many researchers have studied dispersion of various classes of fluids in several geometries and in different time regimes. It has since been shown that the Taylor dispersion coefficient is the long-time asymptotic limit of the generalized dispersion coefficient and is valid only at times that are much greater than the time the solute requires for equilibration in the lateral direction.[2-4] A number of important problems in chemical and biomedical engineering concern geometries with aspect ratios in which the convective timescales for axial flow are

Correspondence concerning this article should be addressed to A. Chauhan at chauhan@che.ufl.edu.

much larger than the lateral equilibration time. In such problems, the Taylor limit of the dispersion coefficient is relevant.

In this paper we determine the Taylor dispersion coefficient in a core–annular geometry where the fluid flow is restricted to the core and the solute diffuses into the solid annulus. Aris first solved this problem by using the method of moments. He developed both the general expressions that are valid for any velocity profile in the core and the annulus and the expression for some special cases, including the case of Poiseuille flow in the core and no-flow in the annulus.[5] Levitt recognized that the core–annular geometry considered by Aris is identical to the geometry of the Krogh cylinder that is used to model the microcirculation and capillary-tissue exchange kinetics. Levitt modeled the capillary-tissue exchange of solutes by using Aris's results and also recognized that in certain cases Aris's model might not be applicable in the capillary-tissue system because of finite capillary lengths and relatively small capillary wall permeabilities to certain solutes. Based on the perturbation approach proposed by Gill and Sankarasubranium,[3] Tepper et al. modified Aris's results to include the time dependency of the dispersion coefficient for plug flow in the capillary.[6] These results can be applied in cases where Aris's results are not valid because of differences between the geometry of the Krogh cylinder and the infinite geometry considered by Aris. In particular, Tepper et al. suggested that for capillary wall permeabilities $\lesssim 10^{-5}$ cm/s, the time dependency of the dispersion coefficient is important, and Aris's results cannot be used. In their analysis, Tepper et al. indicated that the physical significance of the perturbation parameters is not simple and that, for a given set of parameters, it is a priori not clear whether Aris's results are sufficient or the time-dependent coefficients need to be used.

In this paper we obtain the dispersion coefficient for a core–annular geometry with an interfacial mass-transfer resistance by using a perturbation expansion in the aspect ratio. This method allows for easy determination of the regimes in which the results are applicable. We first consider solutes with small interfacial mass-transfer resistance and recover Aris's results. Additionally, we consider the case of large interfacial mass-transfer resistance and show that this problem can also be solved effectively by the method of perturbation expansion in the aspect ratio.

In the next section, the expressions for the average mass-transfer equations are obtained for the entire range of interfacial mass-transfer resistances. Two different velocity profiles in the tube are considered: Poiseuille and plug. Next, for the case of small interfacial mass-transfer resistance, the dispersion coefficients are separated into contributions from effective molecular diffusion, interfacial mass-transfer resistance, and convection. The mechanisms that contribute to each of these are discussed. Asymptotic expressions for the dispersion coefficients are derived to elucidate the various mechanisms and the associated timescales that contribute to dispersion. Additionally, the dispersion coefficient resulting from flow through a channel surrounded on each side by a solid, which is the two-dimensional (2D) equivalent of core–annular flow, is determined. Exact and asymptotic expressions are also derived for this geometry to understand the timescales that lead to the dispersion. Next, the effect of various physical parameters on dispersion is investigated for core–annular Poiseuille flow, and the differences in dispersion between Poiseuille and plug flows are examined. Finally, the relevance of core–annular flow to transport of solutes in the capillaries is discussed, and the theoretical results are compared with some experimental values.

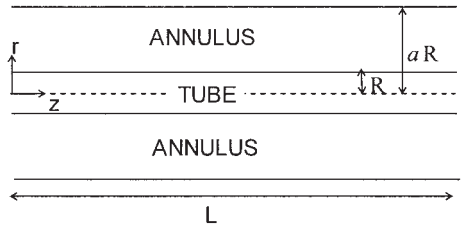

Figure 1. Tube–annulus geometry.

Dispersion Analysis

Governing equations

The core–annular geometry, consisting of a tube surrounded by a solid annulus, is shown in Figure 1. The inner and outer cylinders are of radii R and aR, respectively. The diffusion coefficients of the solute in the fluid and in the solid annulus are D and D_t, respectively.

The transport of solute in the tube and the annulus is governed by the convection–diffusion equations, which are

$$\frac{\partial C}{\partial t} + u_z \frac{\partial C}{\partial z} = D\left[\frac{1}{r}\frac{\partial}{\partial r}\left(r\frac{\partial C}{\partial r}\right) + \frac{\partial^2 C}{\partial z^2}\right] \tag{1}$$

and

$$\frac{\partial C_t}{\partial t} = D_t\left[\frac{1}{r}\frac{\partial}{\partial r}\left(r\frac{\partial C_t}{\partial r}\right) + \frac{\partial^2 C_t}{\partial z^2}\right] \tag{2}$$

In the above equations u_z is the velocity of fluid in the tube in the z-direction, and C and C_t are the solute concentrations in the fluid in the tube and in the annulus, respectively. Herein we assume that there is no convection in the annulus and that the radial flux of the solute at the outer boundary (that is, at $r = aR$) is zero.

Method of solution

Small Interfacial Mass-Transfer Resistance: O(1) Bi. To facilitate solving Eqs. 1 and 2, it is convenient to introduce a pulse of solute at $t = 0$ at a certain spatial location and follow the pulse in time. The pulse moves in the axial direction with a velocity $\bar{u}$ and disperses into a Gaussian shape with a dispersion coefficient D^* (Figure 2). We reformulate the problem in a reference frame moving in the z-direction with a mean velocity $\bar{u}$, so that $z^* = z - \bar{u}t$, where z^* is the axial coordinate in the moving reference frame.

We dedimensionalize the governing equations as follows:

$$\tilde{t} = \frac{tD}{L^2} \qquad \tilde{u}_z = \frac{\langle u\rangle}{u_z} \qquad \tilde{z}^* = \frac{z^*}{L} \qquad \tilde{r} = \frac{r}{R} \qquad \tilde{\bar{u}} = \frac{\bar{u}}{\langle u\rangle}$$

$$\tilde{C} = \frac{C}{C^*} \qquad \tilde{C}_t = \frac{C_t}{C^*} \qquad \tilde{D}^* = \frac{D^*}{D} \tag{3}$$

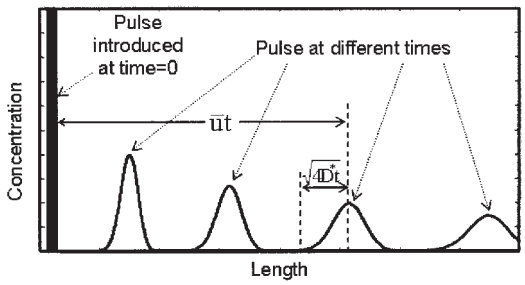

Figure 2. A pulse of solute is introduced at $z = 0$ and then disperses at it travels down the length of the tube.

where L is the length of the tube, R is the radius of the tube, $\langle u \rangle$ is the average velocity of the fluid in the tube, and C^* is a reference concentration. Because we are interested only in the long-time asymptotic limit of the dispersion, time has been dedimensionalized by L^2/D. Additionally, we define a small dimensionless perturbation parameter $\varepsilon = R/L$ and the Peclet number as $\mathrm{Pe} = \langle u \rangle R/D$.

The dimensionless forms of Eqs. 1 and 2 in the moving reference frame are

$$\frac{\partial \tilde{C}}{\partial \bar{t}} + \frac{\mathrm{Pe}}{\varepsilon}(\tilde{u}_z - \tilde{\bar{u}})\frac{\partial \tilde{C}}{\partial \tilde{z}^*} = \frac{1}{\varepsilon^2}\frac{1}{\tilde{r}}\frac{\partial}{\partial \tilde{r}}\left(\tilde{r}\frac{\partial \tilde{C}}{\partial \tilde{r}}\right) + \frac{\partial^2 \tilde{C}}{\partial \tilde{z}^{*2}} \tag{4}$$

and

$$\frac{\partial \tilde{C}_t}{\partial \bar{t}} - \frac{\mathrm{Pe}}{\varepsilon}\tilde{\bar{u}}\frac{\partial \tilde{C}_t}{\partial \tilde{z}^*} = \frac{1}{\varepsilon^2}\frac{D_t}{D}\frac{1}{\tilde{r}}\frac{\partial}{\partial \tilde{r}}\left(\tilde{r}\frac{\partial \tilde{C}_t}{\partial \tilde{r}}\right) + \frac{D_t}{D}\frac{\partial^2 \tilde{C}_t}{\partial \tilde{z}^{*2}} \tag{5}$$

In the above equations, $\tilde{\bar{u}}$ is an unknown constant, which must be found before D^* can be determined. Equations 1 and 2 are subject to the following boundary conditions:

(1) At the center of the tube, $\tilde{r} = 0$, the concentration is finite or, equivalently, $\partial \tilde{C}/\partial \tilde{r} = 0$.

(2) We assume that the tube–annulus interface offers a resistance to solute transport characterized by a mass-transfer coefficient, κ. We neglect solute adsorption at this interface, so that the radial flux of solute is continuous. It follows that the boundary condition at $\tilde{r} = 1$ is $-\partial \tilde{C}/\partial \tilde{r} = -(D_t/D)(\partial \tilde{C}_t/\partial \tilde{r}) = \mathrm{Bi}(K\tilde{C} - \tilde{C}_t)$, where K is the solute's partition coefficient between the tube and surrounding annulus, and Bi is the dimensionless mass-transfer coefficient, given by $\kappa R/D$.

(3) There is no flux out of the annulus at the perimeter of the tube, that is, $\partial \tilde{C}_t/\partial \tilde{r} = 0$ at $\tilde{r} = a$.

Because $\varepsilon \ll 1$, we expand $\tilde{C}$ and $\tilde{C}_t$ in regular expansions as follows:

$$\tilde{C} = \tilde{C}_0 + \varepsilon \tilde{C}_1 + \varepsilon^2 \tilde{C}_2 + \cdots \tag{6}$$

$$\tilde{C}_t = \tilde{C}_{t0} + \varepsilon \tilde{C}_{t1} + \varepsilon^2 \tilde{C}_{t2} + \cdots \tag{7}$$

We now substitute the above expansions into Eqs. 4 and 5, and use the boundary conditions to solve these equations to various orders of ε.

- $O(1/\varepsilon^2)$

To $O(1/\varepsilon^2)$, Eqs. 4 and 5 are

$$0 = \frac{1}{\tilde{r}}\frac{\partial}{\partial \tilde{r}}\left(\tilde{r}\frac{\partial \tilde{C}_0}{\partial \tilde{r}}\right) \tag{8}$$

$$0 = \frac{1}{\tilde{r}}\frac{\partial}{\partial \tilde{r}}\left(\tilde{r}\frac{\partial \tilde{C}_{t0}}{\partial \tilde{r}}\right) \tag{9}$$

Equations 8 and 9 along with the boundary conditions yield $\tilde{C}_{t0} = K\tilde{C}_0$. Thus, the leading order concentrations in the tube and the annulus do not vary in the radial direction and are in equilibrium.

- $O(1/\varepsilon)$

To $O(1/\varepsilon)$, Eqs. 4 and 5 become

$$\mathrm{Pe}(\tilde{u}_z - \tilde{\bar{u}})\frac{\partial \tilde{C}_0}{\partial \tilde{z}^*} = \frac{1}{\tilde{r}}\frac{\partial}{\partial \tilde{r}}\left(\tilde{r}\frac{\partial \tilde{C}_1}{\partial \tilde{r}}\right) \tag{10}$$

$$-\mathrm{Pe}\,\tilde{\bar{u}}\frac{\partial \tilde{C}_{t0}}{\partial \tilde{z}^*} = \frac{D_t}{D}\frac{1}{\tilde{r}}\frac{\partial}{\partial \tilde{r}}\left(\tilde{r}\frac{\partial \tilde{C}_{t1}}{\partial \tilde{r}}\right) \tag{11}$$

The constant $\tilde{\bar{u}}$ is obtained by multiplying Eqs. 10 and 11 by $\tilde{r}$, integrating Eq. 10 from $\tilde{r} = 0$ to $\tilde{r} = 1$, integrating Eq. 11 from $\tilde{r} = 1$ to $\tilde{r} = a$, and then adding the two resulting equations. By following these steps and applying the boundary conditions, we obtain the following equation:

$$\int_0^1 \tilde{u}_z \tilde{r} d\tilde{r} = \frac{1}{2}[1 + K(a^2 - 1)]\tilde{\bar{u}} \tag{12}$$

Because

$$\langle u \rangle \equiv \frac{2\int_0^1 u_z r dr}{R^2}$$

$\int_0^1 \tilde{u}_z \tilde{r} d\tilde{r} = 1/2$, and the dimensionless mean velocity is given by

$$\tilde{\bar{u}} = \frac{1}{1 + K(a^2 - 1)} \tag{13}$$

This result is independent of the velocity profile in the tube. The $\tilde{z}^*$ dependency of Eqs. 10 and 11 can be satisfied by letting $\tilde{C}_1 = B(\tilde{r})(\partial \tilde{C}_0/\partial \tilde{z}^*)$ and $\tilde{C}_{t1} = B_t(\tilde{r})(\partial \tilde{C}_0/\partial \tilde{z}^*)$, where B and B_t are functions of $\tilde{r}$. B and B_t can be determined by substituting the assumed expressions for $\tilde{C}_1$ and $\tilde{C}_{t1}$ into Eqs. 10 and 11 and solving the resulting equations for B and B_t using the appropriate boundary conditions. The resulting expressions for B and B_t are

$$B = -\frac{\mathrm{Pe}\,\tilde{r}^4}{8} + \frac{\mathrm{Pe}}{2}\left\{1 - \frac{1}{2}\left[\frac{1}{1 + K(a^2 - 1)}\right]\right\}\tilde{r}^2 + c_1 \tag{14}$$

$$B_t = \mathrm{Pe}K\frac{D}{D_t}\left[-\frac{\tilde{r}^2}{4(1+K(a^2-1))}+\frac{Ka^4+(1-K)a^2}{2(1+K(a^2-1))^2}\ln(\tilde{r})\right] + c_2 \quad (15)$$

where c_1 and c_2 are constants. Applying the boundary condition that $-\partial B/\partial\tilde{r} = \mathrm{Bi}(KB - B_t)$ at $\tilde{r} = 1$, we obtain the following relationship between the two constants:

$$c_2 = \frac{\mathrm{Pe}K\left(3K(a^2-1)+2\left(\frac{D_t}{D}\right)^{-1}+1\right)}{8(1+K(a^2-1))} + \frac{\mathrm{Pe}K(a^2-1)}{2Bi(1+K(a^2-1))} + Kc_1 \quad (16)$$

The two constants c_1 and c_2 cannot be determined from the last boundary condition ($\tilde{C}_1 = K\tilde{C}_{t1}$ at $\tilde{r} = 1$) because the choice of mean velocity ensures that it is already satisfied; however, separate values of c_1 and c_2 are not needed for the calculation of D^*. If desired, c_1 and c_2 can be determined by using a normalizing condition $\int_0^1 C_1\tilde{r}dr + \int_1^a C_{t1}\tilde{r}dr = 0$, which is equivalent to stating that the total mass in the system at $O(\varepsilon)$ should be zero because the incoming and the outgoing masses at the boundaries are exactly $O(1)$.

- $O(1)$

To $O(1)$ Eqs. 4 and 5 become

$$\frac{\partial\tilde{C}_0}{\partial\tilde{t}} + \mathrm{Pe}(\tilde{u}_z - \tilde{\bar{u}})\frac{\partial\tilde{C}_1}{\partial\tilde{z}^*} = \frac{1}{\tilde{r}}\frac{\partial}{\partial\tilde{r}}\left(\tilde{r}\frac{\partial\tilde{C}_2}{\partial\tilde{r}}\right) + \frac{\partial^2\tilde{C}_0}{\partial\tilde{z}^{*2}} \quad (17)$$

and

$$\frac{\partial\tilde{C}_{t0}}{\partial\tilde{t}} - \mathrm{Pe}\,\tilde{\bar{u}}\frac{\partial\tilde{C}_{t1}}{\partial\tilde{z}^*} = \frac{D_t}{D}\frac{1}{\tilde{r}}\frac{\partial}{\partial\tilde{r}}\left(\tilde{r}\frac{\partial\tilde{C}_{t2}}{\partial\tilde{r}}\right) + \frac{D_t}{D}\frac{\partial^2\tilde{C}_{t0}}{\partial\tilde{z}^{*2}} \quad (18)$$

We substitute for $\tilde{C}_1$ in terms of B, for $\tilde{C}_{t1}$ in terms of B_t, and for $\tilde{C}_{t0}$ as $K\tilde{C}_0$. Next, we multiply both equations by $\tilde{r}$, integrate Eq. 17 from $\tilde{r} = 0$ to $\tilde{r} = 1$, and integrate Eq. 18 from $\tilde{r} = 1$ to $\tilde{r} = a$. Adding the integrated Eqs. 17 and 18 gives

$$\frac{\partial\tilde{C}_0}{\partial\tilde{t}} = \tilde{D}^*\frac{\partial^2\tilde{C}_0}{\partial\tilde{z}^{*2}} \quad (19)$$

where the mean dimensionless dispersion coefficients $\tilde{D}^*$, for Poiseuille flow ($\tilde{D}^*_{po}$) and plug flow ($\tilde{D}^*_{pl}$), are given by

$$\tilde{D}^*_{po} = \frac{D_t}{D} + \frac{11\mathrm{Pe}^2 - 48\frac{D_t}{D} + 48}{48[1+K(a^2-1)]} + \frac{\mathrm{Pe}^2}{24}\frac{\left(\frac{D_t}{D}\right)^{-1}[12\ln(a)-9]a^4 + \left[12\left(\frac{D_t}{D}\right)^{-1}-8\right]a^2 - 3\left(\frac{D_t}{D}\right)^{-1}+8}{(a^2-1)[1+K(a^2-1)]^2} + \frac{\mathrm{Pe}^2}{8}\frac{\left(\frac{D_t}{D}\right)^{-1}[-4\ln(a)+3]a^4 + \left[-4\left(\frac{D_t}{D}\right)^{-1}+1\right]a^2 + \left(\frac{D_t}{D}\right)^{-1}-1}{(a^2-1)[1+K(a^2-1)]^3} + \frac{K\,\mathrm{Pe}^2(a^2-1)^2}{2\mathrm{Bi}[1+K(a^2-1)]^3} \quad (20)$$

and

$$\tilde{D}^*_{pl} = \frac{D_t}{D} + \frac{\mathrm{Pe}^2 - 8\frac{D_t}{D} + 8}{8[1+K(a^2-1)]} + \frac{\mathrm{Pe}^2}{8}\frac{\left(\frac{D_t}{D}\right)^{-1}[4\ln(a)-3]a^4 + \left[4\left(\frac{D_t}{D}\right)^{-1}-2\right]a^2 - \left(\frac{D_t}{D}\right)^{-1}+2}{(a^2-1)[1+K(a^2-1)]^2} + \frac{\mathrm{Pe}^2}{8}\frac{\left(\frac{D_t}{D}\right)^{-1}[-4\ln(a)+3]a^4 + \left[-4\left(\frac{D_t}{D}\right)^{-1}+1\right]a^2 + \left(\frac{D_t}{D}\right)^{-1}-1}{(a^2-1)[1+K(a^2-1)]^3} + \frac{K\,\mathrm{Pe}^2(a^2-1)^2}{2\mathrm{Bi}[1+K(a^2-1)]^3} \quad (21)$$

The above results agree with the results of Aris for Poiseuille flow[5] and that of Levitt for plug flow.[7]

Large Interfacial Mass-Transfer Resistance: O(ε) Bi. We now solve the problem for solutes that have a large interfacial mass-transfer resistance, where $\mathrm{Bi} = \varepsilon\widetilde{\mathrm{Bi}}$. In this case the timescale for transport across the tube–annulus interface (R/κ) is much slower than the timescale for lateral diffusion (R^2/D) but is still faster than the axial diffusion timescale (L^2/D). Accordingly, at the shortest timescale of R^2/D, the tube and the annulus are not expected to be in equilibrium, and the intermediate timescale of R/κ must be introduced into the problem. We do this assuming the concentration in the tube and the annulus are functions of $\tilde{t}_s = \kappa t/R$, $\tilde{t}_l = Dt/L^2$, $\tilde{r} = r/R$, and $\tilde{z} = z/L$. It is noted that this problem is solved in a stationary reference frame. Given that $\tilde{C} = \tilde{C}(\tilde{t}_s, \tilde{t}_l, \tilde{z}, \tilde{r})$ and $\tilde{C}_t = \tilde{C}_t(\tilde{t}_s, \tilde{t}_l, \tilde{z}, \tilde{r})$, it follows that

$$\frac{\partial C}{\partial t} = \frac{D}{L^2}\frac{\partial C}{\partial \tilde{t}_l} + \frac{\kappa}{R}\frac{\partial C}{\partial \tilde{t}_s} \tag{22}$$

and

$$\frac{\partial C_t}{\partial t} = \frac{D}{L^2}\frac{\partial C_t}{\partial \tilde{t}_l} + \frac{\kappa}{R}\frac{\partial C_t}{\partial \tilde{t}_s} \tag{23}$$

Thus, the dimensionless forms of the governing equations Eqs. 1 and 2 are

$$\frac{\partial \tilde{C}}{\partial \tilde{t}_l} + \frac{1}{\varepsilon}\widetilde{\mathrm{Bi}}\frac{\partial \tilde{C}}{\partial \tilde{t}_s} + \frac{\mathrm{Pe}}{\varepsilon}\tilde{u}_z\frac{\partial \tilde{C}}{\partial \tilde{z}} = \frac{1}{\varepsilon^2}\frac{1}{\tilde{r}}\frac{\partial}{\partial \tilde{r}}\left(\tilde{r}\frac{\partial \tilde{C}}{\partial \tilde{r}}\right) + \frac{\partial^2 \tilde{C}}{\partial \tilde{z}^2} \tag{24}$$

and

$$\frac{\partial \tilde{C}_t}{\partial \tilde{t}_l} + \frac{1}{\varepsilon}\widetilde{\mathrm{Bi}}\frac{\partial \tilde{C}_t}{\partial \tilde{t}_s} = \frac{1}{\varepsilon^2}\frac{D_t}{D}\frac{1}{\tilde{r}}\frac{\partial}{\partial \tilde{r}}\left(\tilde{r}\frac{\partial \tilde{C}_t}{\partial \tilde{r}}\right) + \frac{D_t}{D}\frac{\partial^2 \tilde{C}_t}{\partial \tilde{z}^2} \tag{25}$$

The dimensionless boundary conditions are

(1) $\partial \tilde{C}/\partial \tilde{r} = 0$ at $\tilde{r} = 0$

(2) $-\partial \tilde{C}/\partial \tilde{r} = -(D_t/D)(\partial \tilde{C}_t/\partial \tilde{r}) = \varepsilon\widetilde{\mathrm{Bi}}(K\tilde{C} - \tilde{C}_t)$ at $\tilde{r} = 1$

(3) $\partial \tilde{C}_t/\partial \tilde{r} = 0$ at $\tilde{r} = a$

A set of equations for various orders of ε are obtained by substituting the regular expansions of $\tilde{C}$ and $\tilde{C}_t$ into Eqs. 24 and 25 and applying the boundary conditions.

- $O(1/\varepsilon^2)$

To $O(1/\varepsilon^2)$ Eqs. 24 and 25 are

$$0 = \frac{1}{\tilde{r}}\frac{\partial}{\partial \tilde{r}}\left(\tilde{r}\frac{\partial \tilde{C}_0}{\partial \tilde{r}}\right) \tag{26}$$

$$0 = \frac{1}{\tilde{r}}\frac{\partial}{\partial \tilde{r}}\left(\tilde{r}\frac{\partial \tilde{C}_{t0}}{\partial \tilde{r}}\right) \tag{27}$$

Equations 26 and 27 along with the boundary conditions yield $\tilde{C}_{t0} = \tilde{C}_{t0}(\tilde{t}_l, \tilde{t}_s, \tilde{z})$ and $\tilde{C}_0 = \tilde{C}_0(\tilde{t}_l, \tilde{t}_s, \tilde{z})$. This shows that, similar to the small resistance case, the leading order concentrations in the tube and the annulus do not vary in the radial direction; however, these concentrations are no longer in equilibrium as they were in the $O(1)$ Bi case.

- $O(1/\varepsilon)$

To $O(1/\varepsilon)$ Eqs. 24 and 25 are

$$\widetilde{\mathrm{Bi}}\frac{\partial \tilde{C}_0}{\partial \tilde{t}_s} + \mathrm{Pe}\,\tilde{u}_z\frac{\partial \tilde{C}_0}{\partial \tilde{z}} = \frac{1}{\tilde{r}}\frac{\partial}{\partial \tilde{r}}\left(\tilde{r}\frac{\partial \tilde{C}_1}{\partial \tilde{r}}\right) \tag{28}$$

and

$$\widetilde{\mathrm{Bi}}\frac{\partial \tilde{C}_{t0}}{\partial \tilde{t}_s} = \frac{D_t}{D}\frac{1}{\tilde{r}}\frac{\partial}{\partial \tilde{r}}\left(\tilde{r}\frac{\partial \tilde{C}_{t1}}{\partial \tilde{r}}\right) \tag{29}$$

Averaging Eqs. 28 and 29 (that is, multiplying Eqs. 28 and 29 by $\tilde{r}$ and then integrating Eq. 28 from $\tilde{r} = 0$ to $\tilde{r} = 1$ and Eq. 29 from $\tilde{r} = 1$ to $\tilde{r} = a$) and applying the boundary conditions give the following expressions:

$$\frac{\widetilde{\mathrm{Bi}}}{2}\frac{\partial \tilde{C}_0}{\partial \tilde{t}_s} + \frac{\mathrm{Pe}}{2}\frac{\partial \tilde{C}_0}{\partial \tilde{z}} = -\widetilde{\mathrm{Bi}}(K\tilde{C}_0 - \tilde{C}_{t0}) \tag{30}$$

and

$$\left(\frac{a^2 - 1}{2}\right)\frac{\partial \tilde{C}_{t0}}{\partial \tilde{t}_s} = (\mathrm{K}\tilde{\mathrm{C}}_0 - \tilde{\mathrm{C}}_{\mathrm{t0}}) \tag{31}$$

Rearranging Eqs. 30 and 31 to eliminate $\partial \tilde{C}_0/\partial \tilde{t}_s$ and $\partial \tilde{C}_{t0}/\partial \tilde{t}_s$ from Eqs. 28 and 29 gives

$$-2\,\widetilde{\mathrm{Bi}}(K\tilde{C}_0 - \tilde{C}_{t0}) + \mathrm{Pe}(\tilde{u}_z - 1)\frac{\partial \tilde{C}_0}{\partial \tilde{z}} = \frac{1}{\tilde{r}}\frac{\partial}{\partial \tilde{r}}\left(\tilde{r}\frac{\partial \tilde{C}_1}{\partial \tilde{r}}\right) \tag{32}$$

and

$$\frac{2\,\widetilde{\mathrm{Bi}}}{a^2 - 1}(K\tilde{C}_0 - \tilde{C}_{t0}) = \frac{D_t}{D}\frac{1}{\tilde{r}}\frac{\partial}{\partial \tilde{r}}\left(\tilde{r}\frac{\partial \tilde{C}_{t1}}{\partial \tilde{r}}\right) \tag{33}$$

Based on the above differential equations we postulate the following form for $\tilde{C}_1$ and $\tilde{C}_{t1}$:

$$\tilde{C}_1 = \widetilde{\mathrm{Bi}}\,B_2(\tilde{r})(K\tilde{C}_0 - \tilde{C}_{t0}) + \mathrm{Pe}\,B_1(\tilde{r})\frac{\partial \tilde{C}_0}{\partial \tilde{z}} \tag{34}$$

$$\tilde{C}_{t1} = \widetilde{\mathrm{Bi}}\,B_{2t}(\tilde{r})(K\tilde{C}_0 - \tilde{C}_{t0}) \tag{35}$$

Substituting these postulated forms into Eqs. 32 and 33, we obtain the following differential equations for B_1, B_2, and B_{2t}:

$$(\tilde{u}_z - 1) = \frac{1}{\tilde{r}}\frac{\partial}{\partial \tilde{r}}\left(\tilde{r}\frac{\partial B_1}{\partial \tilde{r}}\right) \tag{36}$$

$$-2 = \frac{1}{\tilde{r}}\frac{\partial}{\partial \tilde{r}}\left(\tilde{r}\frac{\partial B_2}{\partial \tilde{r}}\right) \tag{37}$$

$$\frac{2}{a^2 - 1} = \frac{D_t}{D}\frac{1}{\tilde{r}}\frac{\partial}{\partial \tilde{r}}\left(\tilde{r}\frac{\partial B_{2t}}{\partial \tilde{r}}\right) \tag{38}$$

The boundary conditions are $\partial B_1/\partial \tilde{r} = 0$ at $\tilde{r} = 0$, $\partial B_2/\partial \tilde{r} = 0$ at $\tilde{r} = 0$, and $\partial B_{2t}/\partial \tilde{r} = 0$ at $\tilde{r} = a$.

For Poiseuille flow $\tilde{u}_z = -2\tilde{r}^2 + 2$. The above equations can be integrated to give the following results:

$$B_1 = \frac{\tilde{r}^2}{4} - \frac{\tilde{r}^4}{8} + \alpha_3 \tag{39}$$

$$B_2 = \frac{-\tilde{r}^2}{2} + \alpha_1 \tag{40}$$

$$B_{2t} = \left(\frac{D_t}{D}\right)^{-1} \frac{\tilde{r}^2}{2(a^2-1)} - \left(\frac{D_t}{D}\right)^{-1} \frac{a^2}{(a^2-1)} \ln(\tilde{r}) + \alpha_2 \quad (41)$$

where α_1, α_2, and α_3 are constants of integration.

Conservation of mass at $O(\varepsilon)$ requires $\int_0^1 B_1 \tilde{r} d\tilde{r} = 0$ and $\int_0^1 B_2 \tilde{r} d\tilde{r} + \int_1^a B_{2t} \tilde{r} d\tilde{r} = 0$.

Thus,

$$\alpha_1 = (-a^2+1)\alpha_2 + \frac{1}{4}\left(\frac{D_t}{D}\right)^{-1} \times \frac{\{[4\ln(a)-3]a^4 + 2a^2 + 1\}}{a^2-1} + \frac{1}{4} \quad (42)$$

and $\alpha_3 = -1/12$.

- $O(1)$

To $O(1)$ Eqs. 24 and 25 are

$$\frac{\partial \tilde{C}_0}{\partial \tilde{t}_1} + \widetilde{\mathrm{Bi}} \frac{\partial \tilde{C}_1}{\partial \tilde{t}_s} + \mathrm{Pe}\, \tilde{u}_z \frac{\partial \tilde{C}_1}{\partial \tilde{z}} = \frac{1}{\tilde{r}} \frac{\partial}{\partial \tilde{r}} \left(\tilde{r} \frac{\partial \tilde{C}_2}{\partial \tilde{r}} \right) + \frac{\partial^2 \tilde{C}_0}{\partial \tilde{z}^2} \quad (43)$$

and

$$\frac{\partial \tilde{C}_{t0}}{\partial \tilde{t}_1} + \widetilde{\mathrm{Bi}} \frac{\partial \tilde{C}_{t_1}}{\partial \tilde{t}_s} = \frac{D_t}{D} \frac{1}{\tilde{r}} \frac{\partial}{\partial \tilde{r}} \left(\tilde{r} \frac{\partial \tilde{C}_{t2}}{\partial \tilde{r}} \right) + \frac{D_t}{D} \frac{\partial^2 \tilde{C}_{t0}}{\partial \tilde{z}^2} \quad (44)$$

Plugging in for $\partial \tilde{C}_1/\partial \tilde{t}_s$, $\partial \tilde{C}_1/\partial \tilde{z}$, and $\partial \tilde{C}_{t1}/\partial \tilde{t}_s$, and applying the boundary conditions, Eqs. 43 and 44 become

$$\left(-\frac{\mathrm{Pe}^2}{96} - \frac{1}{2} \right) \frac{\partial^2 \tilde{C}_0}{\partial \tilde{z}^2} + \frac{\widetilde{\mathrm{Bi}}\, K\, \mathrm{Pe}}{12} \frac{\partial \tilde{C}_0}{\partial \tilde{z}} - M_1 (K\tilde{C}_0 - \tilde{C}_{t0}) - \frac{\widetilde{\mathrm{Bi}}\, \mathrm{Pe}}{2} \left(\alpha_1 - \frac{1}{6} \right) \frac{\partial \tilde{C}_{t0}}{\partial \tilde{z}} + \frac{1}{2} \frac{\partial \tilde{C}_0}{\partial \tilde{t}_l} = 0 \quad (45)$$

and

$$-\frac{D_t}{D} \frac{(a^2-1)}{2} \frac{\partial^2 \tilde{C}_{t0}}{\partial \tilde{z}^2} + \frac{\mathrm{Pe}\, K\, \widetilde{\mathrm{Bi}}}{6} (3\alpha_1 - 1) \frac{\partial \tilde{C}_0}{\partial \tilde{z}} + M_1 (K\tilde{C}_0 - \tilde{C}_{t0}) + \frac{(a^2-1)}{2} \frac{\partial \tilde{C}_{t0}}{\partial \tilde{t}_l} = 0 \quad (46)$$

where M_1 is a constant given by

$$M_1 = \frac{\widetilde{\mathrm{Bi}}^2}{4} \left\{ K + \left(\frac{D_t}{D}\right)^{-1} \frac{[4\ln(a)-3]a^4 + 4a^2 - 1}{(a^2-1)^2} \right\} \quad (47)$$

Recall, $\tilde{C}_0$ and $\tilde{C}_{t0}$ depend on two timescales, the shorter timescale (t_s) and the longer timescale (t_l). We are now interested in combining the expressions for these two timescales to obtain an expression that is valid at all times. We do this by using Eqs. 22 and 23 to determine the derivatives of the leading order concentrations with respect to the total timescale (t), that is, $\partial \tilde{C}_0/\partial t$ and $\partial \tilde{C}_{t0}/\partial t$. The expressions for $\partial \tilde{C}_0/\partial \tilde{t}_s$ and $\partial \tilde{C}_{t0}/\partial \tilde{t}_s$ are found from Eqs. 30 and 31, and the expressions for $\partial \tilde{C}_0/\partial \tilde{t}_l$ and $\partial \tilde{C}_{t0}/\partial \tilde{t}_l$ are found from Eqs. 45 and 46.

The expression for $\partial \tilde{C}_0/\partial t$ is

$$\frac{\partial \tilde{C}_0}{\partial t} = \frac{D}{L^2} \left[\left(\frac{\mathrm{Pe}^2}{48} + 1 \right) \frac{\partial^2 \tilde{C}_0}{\partial \tilde{z}^2} - \frac{\widetilde{\mathrm{Bi}}\, K\, \mathrm{Pe}}{6} \frac{\partial \tilde{C}_0}{\partial \tilde{z}} + 2M_1 (K\tilde{C}_0 - \tilde{C}_{t0}) + \widetilde{\mathrm{Bi}}\, \mathrm{Pe} \left(\alpha_1 - \frac{1}{6} \right) \frac{\partial \tilde{C}_{t0}}{\partial \tilde{z}} \right] + \frac{\kappa}{R} \left[-2(K\tilde{C}_0 - \tilde{C}_{t0}) - \frac{\mathrm{Pe}}{\widetilde{\mathrm{Bi}}} \frac{\partial \tilde{C}_0}{\partial \tilde{z}} \right] \quad (48)$$

Redimensionalization gives

$$\frac{\partial C_0}{\partial t} = -\left(\frac{\widetilde{\mathrm{Bi}} \varepsilon K}{6} + \langle u \rangle \right) \frac{\partial C_0}{\partial z} + \mathrm{Pe}\kappa \left(\alpha_1 + \frac{1}{6} \right) \frac{\partial C_{t0}}{\partial z} + D \left(\frac{\mathrm{Pe}^2}{48} + 1 \right) \frac{\partial^2 C_0}{\partial z^2} + \left(\frac{2DM_1}{L^2} - \frac{2\kappa}{R} \right) (KC_0 - C_{t0}) \quad (49)$$

The coefficient of $\partial C_0/\partial z$ in Eq. 49 simply reduces to $-\langle u \rangle$ because ε is a small parameter. Similarly, the coefficient of $\partial C_{t0}/\partial z$ can be written as $\langle u \rangle \widetilde{\mathrm{Bi}} \varepsilon [\alpha_1 - (1/6)]$, which is a small quantity and can be neglected. Additionally, the term $2DM_1/L^2$ can be expressed as $(M_1 \varepsilon/\widetilde{\mathrm{Bi}})(2\kappa/R)$ and is therefore negligible in comparison to $2\kappa/R$. The coefficient in front of $(KC_0 - C_{t0})$ can be reduced to $-2\kappa/R$, and Eq. 49 becomes

$$\frac{\partial C_0}{\partial t} + \langle u \rangle \frac{\partial C_0}{\partial z} = D \left(1 + \frac{\mathrm{Pe}^2}{48} \right) \frac{\partial^2 C_0}{\partial z^2} - \frac{2\kappa}{R} (KC_0 - C_{t0}) \quad (50)$$

By a similar approach the equation for $\partial C_{t0}/\partial t$ becomes

$$\frac{\partial C_{t0}}{\partial t} = D_t \frac{\partial^2 C_{t0}}{\partial z^2} + \frac{2\kappa}{R(a^2-1)} (KC_0 - C_{t0}) \quad (51)$$

The above derivation was for the case of Poiseuille flow. For the case of plug flow and $O(\varepsilon)$ Bi, the average equations are the same as Eqs. 50 and 51 except that in Eq. 50 the term $\mathrm{Pe}^2/48$ is eliminated.

Results and Discussion

Range of validity of the average equations

Because the average equations have been derived by using regular expansion, it is clear that all the results are strictly valid only if each of the dimensionless parameters is $O(1)$, that is, they should be much smaller than $1/\varepsilon$ and much larger than ε. Furthermore, if any parameter becomes too small or too large, it should be scaled by the appropriate order in ε. To demonstrate this, let us consider the case of a typical capillary with a κ value of 10^{-7} m/s. As noted by Tepper et al., the results of Aris are no longer accurate for this value of κ.[6] The typical capillary radius is about 5 μm and the typical capillary length is about 1 mm. Thus, the value of ε is about 5×10^{-3}. Using a value of 10^{-9} m^2/s for D, a κ value of 10^{-7} m/s corresponds to a Bi value of 0.5×10^{-3}, which is clearly $O(\varepsilon)$. Thus, it is

clear that Aris's results will not be valid for this value of κ. Instead the average equations for $O(\varepsilon)$ Bi that are derived herein can be used to determine the concentration profiles.

Dispersion coefficient for large permeability: O(1) Bi

To investigate the dependency of $\tilde{D}^*$ on the parameters Pe, Bi, K, a, and D_t/D, it is useful to separate $\tilde{D}^*$ into the contributions from effective molecular diffusivity ($\tilde{D}_0^*$), from the interfacial resistance to mass transfer ($\tilde{D}_R^*$), and from convection ($\mathrm{Pe}^2\tilde{D}_c^*$) as follows:

$$\tilde{D}^* = \tilde{D}_0^* + \tilde{D}_R^* + \mathrm{Pe}^2\tilde{D}_c^* \tag{52}$$

We note that the expressions for $\tilde{D}_0^*$ and $\tilde{D}_R^*$ are the same for both Poiseuille flow and plug flow. The dimensionless quantities in Eq. 52 can be converted to the dimensional form by multiplying them by D.

(1) Contribution to Dispersion from Molecular Diffusivity ($\tilde{D}_0^*$). For both Poiseuille flow and plug flow, $\tilde{D}_0^*$ is given by

$$\tilde{D}_0^* = \frac{D_t}{D} + \frac{1 - \dfrac{D_t}{D}}{1 + K(a^2 - 1)} \tag{53}$$

As $K(a^2 - 1)$ approaches infinity, there is no annulus surrounding the tube, and $\tilde{D}_0^*$ will approach D_t/D. Alternatively, as $K(a^2 - 1)$ approaches 0, the tube is of a negligible size compared to the annulus, and $\tilde{D}_0^*$ will approach 1. Thus, D_0^*, the dimensional $\tilde{D}_0^*$ varies from D to D_t as $K(a^2 - 1)$ varies from 0 to infinity.

(2) Contribution to Dispersion from Interfacial Resistance ($\tilde{D}_R^*$). The dispersion caused by the interfacial resistance, $\tilde{D}_R^*$, is given by

$$\tilde{D}_R^* = \frac{K\,\mathrm{Pe}^2(a^2 - 1)^2}{2\mathrm{Bi}[1 + K(a^2 - 1)]^3} \tag{54}$$

$\tilde{D}_R^*$ is expected to depend only on the mean velocity, $\langle u \rangle$, and not on the velocity profile. To determine whether this is the case, we obtain the dispersion coefficient for the same geometry in the limiting case when both the fluid in the tube and the solid annulus are radially well mixed. In this limit, the dimensionless governing equations for the tube and the annulus are

$$\frac{\partial \tilde{C}}{\partial \tilde{t}} + \frac{\mathrm{Pe}}{\varepsilon}(1 - \tilde{\tilde{u}})\frac{\partial \tilde{C}}{\partial \tilde{z}^*} = -\frac{2\,\mathrm{Bi}}{\varepsilon^2}(K\tilde{C} - \tilde{C}_t) + \frac{\partial^2 \tilde{C}}{\partial \tilde{z}^{*2}} \tag{55}$$

and

$$\frac{\partial \tilde{C}_t}{\partial \tilde{t}} - \frac{\mathrm{Pe}}{\varepsilon}\tilde{\tilde{u}}\frac{\partial \tilde{C}_t}{\partial \tilde{z}^*} = \frac{2\,\mathrm{Bi}}{(a^2 - 1)\varepsilon^2}(K\tilde{C} - \tilde{C}_t) + \frac{D_t}{D}\frac{\partial^2 \tilde{C}_t}{\partial \tilde{z}^{*2}} \tag{56}$$

The above equations are also solved by the regular expansion method to different orders in ε to determine the mean velocity and the dispersion coefficient. The results to different orders are

$$O(\varepsilon^0)\text{: } \tilde{C}_0 = \tilde{C}_0(\tilde{z}, \tilde{t}) \qquad \text{and} \qquad \tilde{C}_{t,0} = \tilde{C}_{t,0}(\tilde{z}, \tilde{t})$$

$$O(\varepsilon^1)\text{: } \tilde{\tilde{u}} = \frac{1}{1 + K(a^2 - 1)} \qquad \text{and}$$

$$\mathrm{Pe}\frac{\partial \tilde{C}_0}{\partial \tilde{z}} = -2\,\mathrm{Bi}(K\tilde{C}_1 - \tilde{C}_{t,1})$$

$$O(\varepsilon^2)\text{: } \frac{\partial \tilde{C}_0}{\partial \tilde{t}} = (\tilde{D}_R^* + \tilde{D}_0^*)\frac{\partial^2 \tilde{C}}{\partial \tilde{z}^{*2}}$$

Thus, the dispersion coefficient for the case of a radially well mixed tube and annulus is simply the sum of the contributions to dispersion from diffusion and interfacial mass-transfer resistance. This shows that $\tilde{D}_R^*$ is simply an additive term that does not depend on the velocity profile.

(3) Contribution to Dispersion from Convection ($\tilde{D}_c^*$). $\tilde{D}_c^*$ is the only term that is affected by the velocity profile. For Poiseuille flow it is given by

$$\tilde{D}_c^* = \frac{\left\{11K^2 + \left(\dfrac{D_t}{D}\right)^{-1} K[24\,\ln(a) - 18]\right\}a^4 + \left\{-22K^2 + K\left[24\left(\dfrac{D_t}{D}\right)^{-1} + 6\right]\right\}a^2 + 11K^2 - 6K\left[\left(\dfrac{D_t}{D}\right)^{-1} + 1\right] + 1}{48[1 + K(a^2 - 1)]^3} \tag{57}$$

Below we discuss the physical mechanisms that contribute to $\tilde{D}_c^*$ and the dependency of $\tilde{D}_c^*$ on various parameters. These discussions are limited to Poiseuille flow, although the differences in dispersion between the Poiseuille flow and the plug flow are discussed later in the article.

Mechanism of Dispersion. The mechanism of dispersion that leads to $\tilde{D}_c^*$ for Poiseuille flow is illustrated in Figure 3. Once a pulse of solute is introduced into the tube, it spreads into the annulus (Figure 3a). The flow inside the tube then stretches the pulse into a paraboloid, creating radial concentration gradients (Figure 3b). Accordingly, the solute diffuses from the tube to the annulus at the front end of the pulse and from the annulus to the tube at the back end. After neglecting interfacial mass-transfer resistance, there are four timescales that are involved in the process described above: (1) τ_1, the timescale for transfer of solute from the tube to the annulus at the front end of the parabaloid; (2) τ_2, the timescale for transfer of solute from the annulus to the tube at the back end of the parabaloid; (3) τ_3, the timescale for radial diffusion within the tube; and (4) τ_4, the timescale for radial diffusion within the annulus.

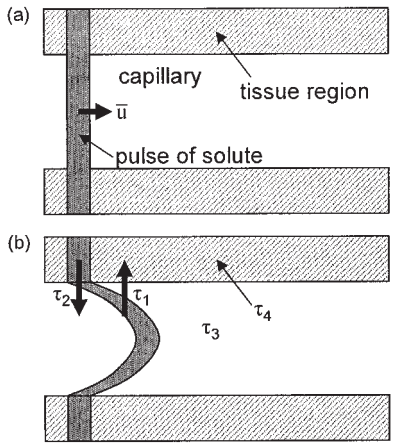

Figure 3. (a) A pulse of solute is introduced into the tube, which immediately spreads into the annular region. (b) The pulse of solute acquires a parabolic shape as a result of convection inside the tube and the solute diffuses as a result of concentration gradients.

Each of the four timescales discussed above contributes to the dispersion, and it is useful to determine their scalings. Before we do this, let us point out that the dimensional convective contribution to the dispersion coefficient is $\mathrm{Pe}^2\tilde{D}_c^*$, which scales as $l^2/\Delta t$, where l is the axial distance traveled by a pulse during Δt, so that $1 \sim \bar{u}\Delta t$. It follows that

$$\mathrm{Pe}^2 D_c^* \sim \bar{u}^2\Delta t = \frac{\langle u\rangle^2}{[1 + K(a^2 - 1)]^2}\,\Delta t$$

Because, to leading order, the concentrations in the tube and the annulus are in equilibrium, the appropriate Δt is the time needed to achieve equilibrium in the radial direction. This Δt is essentially the sum of the four timescales that are discussed above. We now determine the scalings for each of these four timescales for Poiseuille flow.

The timescales τ_3 and τ_4 are simply R^2/D and $[R^2(a - 1)^2]/D_t$, respectively. To determine τ_1, we first find the mass of the solute that diffuses from the tube to the annulus at the front end of the paraboloid. At the front end of the parabaloid, the concentration in the annulus changes from approximately zero to KC, where C is the concentration scale in the tube. Accordingly, the mass transferred between the tube and annulus at the front end of the parabaloid per unit length is $KC\pi R^2(a^2 - 1)$. The radial solute flux in the tube scales as DC/R, so the solute transport in the tube per unit length is DC. τ_1 is the ratio of these two quantities, that is, $[KR^2(a^2 - 1)]/D$. To determine τ_2, we first find the mass that diffuses from the annulus to the tube at the back end. Because the tube and the annulus are always in equilibrium, this is equal to the mass that diffuses from the tube to the annulus at the front end, $KC\pi R^2(a^2 - 1)$. The diffusive flux from the annulus to the tube scales as $D_tKC/[R(a - 1)]$. Accordingly, the solute transport in the annulus per unit length is $D_tKC/(a - 1)$. τ_2 scales as the ratio of these two quantities, $[R^2(a - 1)^2(a + 1)]/D_t$. The contribution to D_c^* from each of the four timescales becomes amply evident in the asymptotic expressions for $\tilde{D}_c^*$, which are found below.

Asymptotic Limits of $\tilde{D}_c^*$. The derivation above assumes that all the dimensionless parameters (a, K, and D_t/D) are $O(1)$ quantities in ε. Thus, in the asymptotic expansions of the Poiseuille flow $\tilde{D}_c^*$ below, the large and the small quantities are supposed to be $<1/\varepsilon$ and $>\varepsilon$, respectively. Below we obtain the asymptotic expressions and also identify the timescale that dominates the dispersion in each case.

The expression for $\tilde{D}_c^*$ is linear in $(D_t/D)^{-1}$, so the asymptotes for small and large values of D_t/D are obvious. As D_t/D approaches 0, the dominant timescales are τ_2 and τ_4, which contribute to the term proportional to D_t/D. For large D_t/D, the dominant timescales are τ_1 and τ_3, which contribute to the term independent of D_t/D.

In the limit of a approaching 1, the asymptotic result obtained by expanding Eq. 57 is

$$\lim_{a\to 1}\tilde{D}_c^* \cong \frac{1}{48} + \frac{K(a-1)}{8} \tag{58}$$

In the limit of K approaching 0, the asymptotic result obtained by expanding Eq. 57 is

$$\lim_{K\to 0}\tilde{D}_c^* \cong \frac{1}{48} + \left\{\frac{1}{2}\left(\frac{D_t}{D}\right)^{-1}\left[\ln(a) - \frac{3}{4}\right]a^4 + \frac{1}{2}\left[\left(\frac{D_t}{D}\right)^{-1} + \frac{1}{8}\right]a^2 - \frac{1}{8}\left[\left(\frac{D_t}{D}\right)^{-1} + \frac{1}{2}\right]\right\}K \tag{59}$$

In both of the above cases the longest timescale is τ_3, which contributes to the leading order term for $\tilde{D}_c^*$ in the above expressions. This term is identical to the dispersion coefficient for flow through a tube.[5] Thus, the dispersion coefficient in our system reduces to that for flow through a tube as the thickness of the annulus ($a - 1$) or the partition coefficient (K) approaches zero. Equation 57 is valid only when $K < [1/(a^4\ln a)](D_t/D)$, so the region of validity becomes small as the value of a increases.

For the limit of $\tilde{D}_c^*$ as K approaches infinity, the longest timescale is τ_1. Because the mean velocity scales as $1/K$ and Δt scales as K, $\tilde{D}_c^*$ scales as $1/K$. The exact expression for $\tilde{D}_c^*$ as K approaches infinity is

$$\lim_{K\to\infty}\tilde{D}_c^* \cong \frac{11a^4 - 22a^2 + 11}{48(a^2 - 1)^3 K} \tag{60}$$

As a becomes large, the mean velocity scales as $1/a^2$, and τ_2 scales as a^3. The dispersion coefficient is thus expected to scale as $1/a$; however, the exact expansion shows that $\tilde{D}_c^*$ scales as $\ln(a)/a^2$.

$$\lim_{a\to\infty}\tilde{D}_c^* \cong \frac{1}{48}\,\frac{11K^2 + 24\left(\frac{D_t}{D}\right)^{-1}\ln(a)\,K - 18\left(\frac{D_t}{D}\right)^{-1}K}{K^3a^2} + O\left(\frac{1}{a^4}\right) \tag{61}$$

The cylindrical curvature of the tube–annulus geometry was neglected while determining the scalings and that may be the

reason for the disagreement between the scaling and the exact expansion as a becomes large. To verify that neglect of the cylindrical curvature led to this discrepancy, we find the dispersion coefficient for Poiseuille flow in the 2D equivalent of core–annular flow, that is, 2D planar fluid flow in a channel of height $2h$ surrounded by a solid of thickness $(a-1)h$. We also develop scalings and the exact solutions for this geometry.

Flow through a Channel. The results for flow through a channel, neglecting interfacial mass-transfer resistance, are as follows:

$$\tilde{\bar{u}} = \frac{1}{1 + K(a-1)} \tag{62}$$

$$\tilde{D}^* = \frac{D_t}{D} + \frac{17\mathrm{Pe}^2 - 35\dfrac{D_t}{D} + 35}{35[1 + K(a-1)]} + \frac{\mathrm{Pe}^2}{15}\frac{5\dfrac{D_t}{D}(a^2 - 10a + 5) - 12}{[1 + K(a-1)]^2} + \frac{\mathrm{Pe}^2}{3}\frac{\dfrac{D_t}{D}(-a^2 + 2a - 1) + 1}{[1 + K(a-1)]^3} \tag{63}$$

The timescales for equilibration in the channel and in the surrounding solid are $\tau_3 = h^2/D$ and $\tau_4 = [(a-1)^2h^2]D_t$. For a channel width W, the mass transferred per unit length is $KC(a-1)hW$. The lateral flux in the solid scales as DC/h and, accordingly, the solute transport per unit length is DC/hW. τ_1 scales as the ratio of these two quantities, $K(a-1)(h^2/D)$. The mass that diffuses from the annulus to the tube at the back end is equal to the mass that diffuses from the tube to the annulus at the front end, and is thus equal to $KC(a-1)hW$. The diffusive flux from the annulus to the tube scales as $D_tKC/[R(a-1)]$. Accordingly, the solute transport per unit length is $D_tKC/(a-1)$. τ_2 scales as the ratio of these two quantities, $[(a-1)^2h^2]/D_t$. Thus, for the planar problem both τ_2 and τ_4 are the same.

Similar to previous cases, the dispersion coefficient is linear in $(D_t/D)^{-1}$. As D_t/D approaches 0, the dominant timescales are τ_2 and τ_4, and for large D_t/D, the dominant timescales are τ_1 and τ_3.

The asymptotic expressions of $\tilde{D}_c^*$ for Poiseuille flow in this geometry for large and small values of a and K are

$$\lim_{a\to 1}\tilde{D}_c^* \cong \frac{2}{105} + \frac{4K(a-1)}{35} \tag{64}$$

$$\lim_{a\to\infty}\tilde{D}_c^* \cong \frac{\left(\dfrac{D_t}{D}\right)^{-1}}{3K^2} + \frac{\left(\dfrac{D_t}{D}\right)^{-1}\left[-\dfrac{1}{3K^3} + \dfrac{2(K-1)}{3K^3} - \dfrac{2}{3K^2} + \dfrac{17}{35K}\right]}{a} \tag{65}$$

$$\lim_{K\to 0}\tilde{D}_c^* \cong \frac{2}{105} + \left[\left(\frac{D_t}{D}\right)^{-1}\left(\frac{1}{3}a^3 - a^2 + a - \frac{1}{3}\right) + \frac{4}{35}a - \frac{4}{35}\right]K \tag{66}$$

$$\lim_{K\to\infty}\tilde{D}_c^* \cong \frac{17}{35(a-1)K} \tag{67}$$

As a approaches infinity the dominant timescale is τ_2 and the convective contribution to dispersion, $\tilde{D}_c^*$, scales as

$$\bar{u}^2\tau_2 \sim \frac{(a-1)^2h^2}{D_t}\frac{\langle u\rangle^2}{[1 + K(a-1)]^2} \sim D\frac{\langle u\rangle^2h^2}{D^2}\left(\frac{D_t}{D}\right)^{-1}\frac{1}{K^2} \sim \frac{D\,\mathrm{Pe}^2}{K^2}\left(\frac{D_t}{D}\right)^{-1}$$

This matches the asymptotic scaling given in Eq. 65. Similarly, as a approaches 1, the dominant timescale is τ_3 and

$$\bar{u}^2\tau_3 \sim \frac{h^2}{D_t}\frac{\langle u\rangle^2}{[1 + K(a-1)]^2} \sim D\,\mathrm{Pe}^2$$

which matches the asymptotic scaling given in Eq. 64. As K approaches infinity, the dominant scale is τ_1 and

$$\bar{u}^2\tau_1 \sim \frac{K(a-1)h^2}{D_t}\frac{\langle u\rangle^2}{[1 + K(a-1)]^2} \sim \frac{D\,\mathrm{Pe}^2}{K(a-1)}$$

which is the same as the asymptotic limit obtained in Eq. 67. As K approaches zero, both τ_3 and τ_4 are of the same order; however, τ_4 does not contribute to dispersion because in this limit, to leading order, no solute diffuses into the annulus. Accordingly, only τ_3 is the dominant timescale and

$$\bar{u}^2\tau_3 \sim \frac{h^2}{D_t}\frac{\langle u\rangle^2}{[1 + K(a-1)]^2} \sim D\,\mathrm{Pe}^2$$

which matches the asymptotic scaling from Eq. 66. It follows that this simple scaling analysis can indeed predict the asymptotic forms of the dispersion coefficient; however, in the scaling analysis for the cylindrical tube–annulus geometry, curvature effects were neglected and that caused a discrepancy between the scaling analysis and asymptotic expansion for $\tilde{D}_c^*$ in the limit of large a.

Dependency of $\tilde{D}_c^*$ on Parameters. The dependency of $\tilde{D}_c^*$ on a, K, and D_t/D for the case of cylindrical Poiseuille flow surrounded by the solid annulus is illustrated in Figures 4–6. Figure 4 shows the dependency of $\tilde{D}_c^*$ on a for four different values of K. At $a = 1$, $\tilde{D}_c^*$ goes to 1/48, as is expected from the asymptotic results. Although not evident in the graph for all values of K, $\tilde{D}_c^*$ increases linearly with a slope of $K/8$ as a becomes >1. As a becomes large, $\tilde{D}_c^*$ decreases as $\ln(a)/a^2$. Accordingly, there is a maximum value of $\tilde{D}_c^*$ for an intermediate value of a, which is larger for smaller K values. The values of a at which the maxima are reached become smaller on increasing K. In fact for K values of 10 and 100, the maxima are not evident in the figure because they occur at very small a values.

Figure 5 shows the dependency of $\tilde{D}_c^*$ on K for different values of D_t/D. These curves show the linear dependency of $\tilde{D}_c^*$ for small K values and the $1/K$ dependency for large K values, as evident by slopes of 1 and -1, respectively, on the log–log plot. The region of linear behavior in the small K regime is restricted to very small K values for D_t/D values of 10 and 100, and accordingly the linear regime is not visible in the figure for

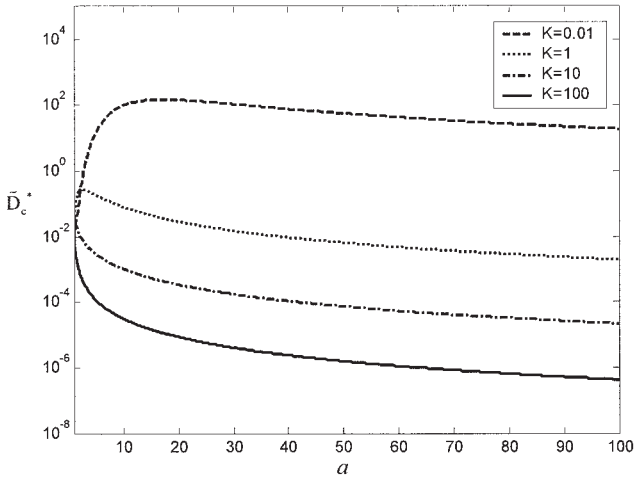

Figure 4. $\tilde{D}_c^*$ for Poiseuille flow vs. a for different K values where $D_t/D = 0.1$.

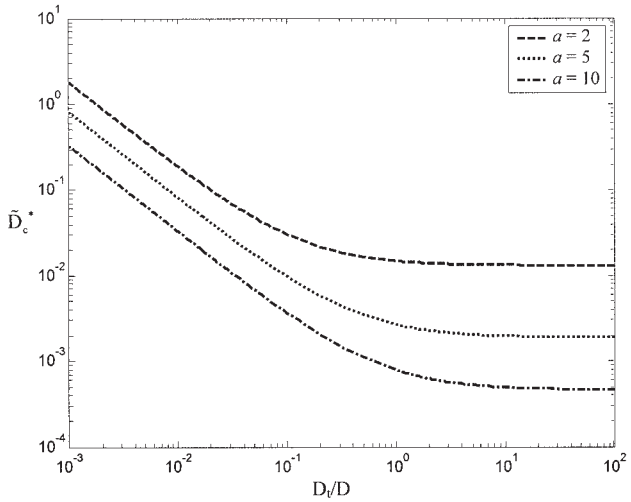

Figure 6. $\tilde{D}_c^*$ for Poiseuille flow vs. D/D_t for different a values where $K = 5$.

these two cases. It is noted that our analysis is strictly valid for $\tilde{D}_c^*$ values that are $O(1)$ in ε. Thus, in the small K and large a regimes, the trends shown in Figures 4 and 5 are valid only for long tubes, which correspond to very small ε values. As expected, $\tilde{D}_c^*$ approaches 1/48 as K approaches 0.

Figure 6 illustrates the behavior of $\tilde{D}_c^*$ as a function of D_t/D for three different values of a. $\tilde{D}_c^*$ behaves as $(D_t/D)^{-1}$ in the small D_t/D regime, as evident by a slope of -1 on the log–log plot and approaches a constant value as D_t/D approaches infinity.

Effect of Velocity Profile in the Tube on Dispersion. The difference between the dispersion coefficients for Poiseuille flow (Eq. 20) and plug flow (Eq. 21) is given by

$$\tilde{D}_{po}^* - \tilde{D}_{pl}^* = \frac{\mathrm{Pe}^2[1 + 5K(a^2 - 1)]}{48[1 + K(a^2 - 1)]^2} \tag{68}$$

Interestingly, the difference is independent of the solute's diffusivity in the annulus. Each of the four timescales discussed above for Poiseuille flow is also pertinent to plug flow. Thus, qualitatively, the dependency of $\tilde{D}^*$ on various parameters for plug flow is similar to that for Poiseuille flow. The ratio of the convective contribution of $\tilde{D}_{pl}^*$ (denoted $\tilde{D}_{c\,pl}^*$) to the convective contribution of $\tilde{D}_{po}^*$ (denoted $\tilde{D}_{c\,po}^*$) is shown as a function of a in Figure 7. This ratio is zero for $a = 1$ because there is no convective contribution to dispersion for plug flow in this limit. The ratio then increases with increasing a and levels off at values that range from about 0.5 to 1 for a wide range of K. The value of the ratio at large a varies inversely with K.

Dispersion coefficient for small permeability: O(ε) Bi

The expressions for the dispersion coefficient given by Eqs. 20 and 21 become unbounded as Bi approaches zero. This is clearly an incorrect result because, as the interfacial mass-transfer resistance approaches infinity, the mass-transfer problem should reduce to the classical problem of Taylor dispersion in a tube. This suggests that Eqs. 20 and 21 are not uniformly valid. On scaling Bi as $O(\varepsilon)$, the average equations reduce to Eqs. 50 and 51, which represent a set of two coupled partial differential

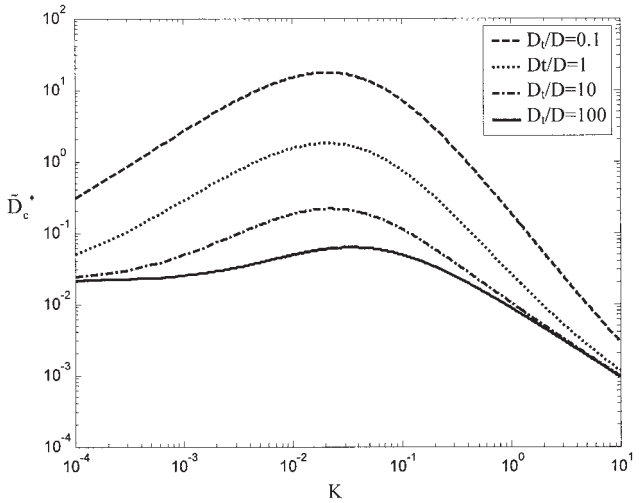

Figure 5. $\tilde{D}_c^*$ for Poiseuille flow vs. K for different D_t/D values where $a = 5$.

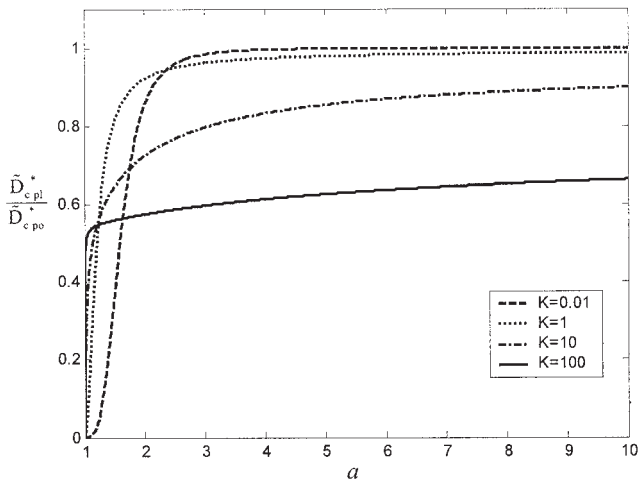

Figure 7. Ratio of $\tilde{D}_c^*$ for plug and Poiseuille flow vs. a for different K values where $D/D_t = 10$.

equations. The equation for the tube essentially becomes identical to flow through a tube with a source term that accounts for the mass loss to the annulus. The annulus equation is similar except that there is no effect of convection. Also, on taking the limit as Bi goes to zero, the tube equation correctly becomes identical to the problem of flow through a tube.

The set of coupled equations can be combined to yield the following differential equation for the tube concentration:

$$\frac{R}{2\kappa}\frac{\partial^2 C_0}{\partial t^2}+\left(K-\frac{1}{(a^2-1)}\right)\frac{\partial C_0}{\partial t}-\frac{R}{2\kappa}\left(D\left(1+\frac{Pe^2}{48}\right)+D_t\right)\frac{\partial^2}{\partial z^2}\frac{\partial C_o}{\partial t}+\frac{\langle u\rangle R}{2\kappa}\frac{\partial}{\partial z}\frac{\partial C_o}{\partial t}=-\frac{D_t DR}{2\kappa}\left(1+\frac{Pe^2}{48}\right)\frac{\partial^4 C_0}{\partial z^4}+\frac{D_t\langle u\rangle R}{2\kappa}\frac{\partial^3 C_0}{\partial z^3}+\left(KD_t-\frac{D}{(a^2-1)}\left(1+\frac{Pe^2}{48}\right)\right)\frac{\partial^2 C_0}{\partial z^2}+\frac{\langle u\rangle}{(a^2-1)}\frac{\partial C_o}{\partial z} \quad (69)$$

Following the approach of Subramanian and Gill,[4] we use the following expansion:

$$\frac{\partial C_0}{\partial t}=\beta_1\frac{\partial C_0}{\partial z}+\beta_2\frac{\partial^2 C_0}{\partial z^2}+\beta_3\frac{\partial^3 C_0}{\partial z^3}+\cdots \quad (70)$$

By substituting the above expansion in Eq. 69, the various coefficients can be determined. The resulting expressions for these coefficients are:

$$\beta_1=-\frac{\langle u\rangle}{1+K(a^2-1)} \quad (71)$$

$$\beta_2=\frac{D\left(1+\frac{\mathrm{Pe}^2}{48}\right)+KD_t(a^2-1)}{[1+K(a^2-1)]}+\frac{K\,\mathrm{Pe}^2D(a^2-1)^2}{2\,\mathrm{Bi}[1+K(a^2-1)]^3} \quad (72)$$

$$\beta_3=\frac{\mathrm{Pe}^3KRD(a^2-1)^3}{4\,\mathrm{Bi}^2(1+K(a^2-1))^5}(1-K(a^2-1))+\frac{\mathrm{Pe}R(a^2-1)}{2Bi}\left(\frac{2D\left(1+\frac{\mathrm{Pe}^2}{48}\right)+KD_t(a^2-1)}{(1+K(a^2-1))^3}-\frac{2D\left(1+\frac{\mathrm{Pe}^2}{48}\right)}{(1+K(a^2-1))^2}+\frac{D_t}{(1+K(a^2-1))}\right) \quad (73)$$

As is shown by the equations, β_1 is independent of Bi and is simply the mean velocity of the solute for the case of $O(1)$ Bi. Also β_2 can be interpreted as the dispersion coefficient and the contribution to dispersion from axial diffusion (D_0^*) and from the interfacial resistance (D_R^*) are identical to those for the case of O(1) Bi. However, β_2 and β_3 behave as 1/Bi and 1/Bi^2, respectively. Thus, the contribution from the higher order terms is very large at small Bi. This shows that series given by Eq. 70 does not converge for $O(\varepsilon)$ Bi. The average equations cannot be expressed as a single convection–dispersion equation, and Eqs. 50 and 51 need to be solved simultaneously to predict the average concentration profiles in the tube and the annulus.

Applications to Transport in Tissues

Exchange of nutrients, drugs, and other solutes between vascular and tissue regions occurs in the capillaries by transport across the capillary wall. In most capillary-transport models it is commonly assumed that each capillary supplies nutrients to an annular tissue region around the capillary, referred to as the *Krogh tissue cylinder*.[8-10] As noted by a number of researchers (Tepper et al.,[6] Levitt,[7] and others), the problem explored in this paper can be thought of as a blood capillary surrounded by a Krogh tissue cylinder. Our model is thus of relevance for understanding and quantifying dispersion of solutes in the capillary blood vessels, which is important in the fields of physiology, toxicology, and pharmacokinetics.

Although the geometry of our model mimics the Krogh tissue cylinder, a number of our assumptions are not consistent with the physiological conditions in the capillaries. It is well known that blood is a non-Newtonian fluid and that the blood flow through the blood vessels is best described by a Casson fluid model.[11] The velocity profiles (Poiseuille and plug) used in our model do not accurately represent the blood flow in the capillaries. In blood flow through the capillary, the tube diameter is smaller than the size of the red blood cells (RBCs). Consequently, the RBCs must deform to flow through the capillaries. Plasma fills the space between successive RBCs, and there is an extremely thin layer of plasma between the RBCs and the capillary wall. Blood flow inside the capillaries is similar to plug flow; however, the region between successive RBCs is kept well mixed by a pair of counterrotating vortices that convect with the flow.[11-13] Aside from the velocity profiles, there are a number of other important issues that have been neglected from our model, such as convective flow of blood into the tissue (filtration), geometric factors (such as variations in capillary length and diameter), protein binding, and consumption of solutes by reactions. Thus, our model cannot be directly applied to quantify dispersion in the tissues; however, it elucidates some of the important mechanisms that lead to dispersion. Our current model may be more valid to assess dispersion in isolated organ experiments, in which a buffer solution may be used in place of blood.[14-17] In such a case, RBCs are not present, and thus the fluid velocity profile is expected to be Poiseuille.

Although, for the reasons mentioned above, our model predictions are not expected to match the experimentally measured values of dispersion coefficients in the capillaries of tissues, it is nonetheless useful to make such a comparison. This allows us to gauge the importance of the proposed mechanisms in causing dispersion in the capillaries. Below we compare the calculated dispersion coefficients for both Poiseuille flow and plug flow for the $O(1)$ Bi case, neglecting interfacial mass-transfer resistance, with those experimentally determined in animal tissues.

Comparison of $\tilde{D}^*$ Values with Experimental Values

Oliver et al. included dispersion in a whole-body pharmacokinetic model, in which they characterize the dispersion in the tissues by a parameter D_N.[18] They reviewed a number of experimental studies and determined D_N for the drug cyclosporine in a

Table 1. Comparison of Tissue Dispersion Numbers Predicted from Our Model to Experimentally Determined Values for Cyclosporine in a Rat

Tissue	K‡	Q‡ (mL/min)	V‡ (mL)	a	R (μm)	D_N**	D_N^* Poiseuille Flow	D_N^* Plug Flow
Lungs	5.70	44.50	1.60	10.00	5.00	0.60	1.91	1.79
Muscle	1.30	6.80	125.60	3.06†	3.61†	3.00	2.80	1.96
Skin	3.90	4.50	43.80	10.00	5.00	12.00	2.60	2.60
Adipose	13.90	1.80	10.00	11.28†	3.02†	12.00	5.18	5.28
Kidney	7.43	14.27	2.00	2.80†	3.01†	0.48	0.09	0.09
Liver	12.43	14.70	11.00	3.03†	2.87†	0.60	0.68	0.68

$D_t/D = 0.1$, $L = 0.3$ mm, $D = 10^{-9}$ m^2/s.
‡From Oliver et al.[18]
†Calculated using information from Altman.[22]

250 g rat. We neglect capillary wall resistance and calculate $\tilde{D}^*$ for cyclosporine in a rat from Eqs. 20 and 21. These values are then compared to those determined by Oliver et al. Although values of the flow rates (Q), tissue volumes (V), and partition coefficients (K) for cyclosporine in a rat are given in the literature,[18] the values of parameters a, D, D_t, R, and L are not. We therefore assume L to be 0.3 mm[19] and D_t/D to be 0.1 in all tissues.[20] Calculation of $\tilde{D}^*$ requires determination of Pe and thus $\langle u \rangle$ for each tissue. The following equation is used to determine $\langle u \rangle$:

$$Q = \pi R^2 \langle u \rangle n_c \tag{74}$$

The volumetric flow rate of blood exiting each tissue (Q), a known parameter, is assumed to be equal to the product of the area of a single capillary (πR^2), $\langle u \rangle$, and the number of capillaries in the tissue (n_c). The number of capillaries in the tissue is found by setting the total volume of the tissue compartment (V) equal to the sum of the volume of the capillaries in that tissue (V_c) and the volume of tissue space in that compartment (V_t). This results in the following equations:

$$V = V_t + V_c = n_c(\pi a^2 R^2 L - \pi R^2 L) + n_c \pi a R^2 L = n_c \pi a^2 R^2 L \tag{75}$$

$$n_c = \frac{V}{\pi a^2 R^2 L} \tag{76}$$

By combining Eqs. 76 and 74, $\langle u \rangle$ is found for each tissue according to the following equation:

$$\langle u \rangle = \frac{Q a^2 L}{V} \tag{77}$$

The parameters a and R were calculated for each tissue from experimentally determined values of capillary number density (n_c/A) and capillary surface area to tissue volume ratio (S_c/V)[21] according to the following equations:

$$R = \frac{1}{2\pi} \frac{S_c}{V} \tag{78}$$

$$a = \frac{1}{R} \sqrt{\frac{1}{\pi} \left(\frac{n_c}{A} \right)^{-1}} \tag{79}$$

These calculated values are used in Eqs. 20 and 21 to find $\tilde{D}^*$ for Poiseuille flow and plug flow. For tissues in which n_c/A and S_c/V data were not available, a was assumed to be 10 and R was assumed to be 5 μm. Because the D_N value proposed by Oliver et al. was dedimensionalized differently than our $\tilde{D}^*$, we use the following relationship to make the comparison with our calculated $\tilde{D}^*$:

$$D_N^* = \frac{D \tilde{D}^* V K}{L^2 Q} \tag{80}$$

To avoid confusion, we have designated our comparable calculated dispersion number as D_N^*, which will be compared to the experimental D_N values for each tissue. The calculated D_N^* values (for both Poiseuille flow and plug flow) and the experimentally measured D_N values are shown in Table 1 , along with the K, V, Q, a, and R values. In most tissues, the model predictions are of the same order as the experimental values, suggesting that the mechanism of dispersion proposed herein may be important in tissues. The Krogh cylinder model is expected to most closely resemble the actual physiology of the muscle,[9] and the agreement is the best for this tissue.

Conclusions

The dispersion of a solute in a core–annular flow with a solid annulus has been studied for both Poiseuille flow and plug flow for small and large interfacial mass-transfer resistances. The dispersion coefficient for small resistance is the sum of contributions from axial diffusion, interfacial mass-transfer resistance, and convection. The contribution from interfacial mass-transfer resistance is independent of the fluid velocity profile. The convective contribution to dispersion arises from four different mechanisms which can be expressed in terms of four timescales: (1) τ_1, the timescale for transfer of solute from the tube to the annulus at the front end of the solute pulse, (2) τ_2, the timescale for transfer of solute from the annulus to the tube at the back end of the solute pulse, (3) τ_3, the timescale for radial diffusion within the tube, and (4) τ_4, the timescale for radial diffusion within the annulus. For the cases of vanishing annulus thickness and small solute solubility in the annulus, the dispersion coefficient becomes the limit of that for flow through a tube. The dispersion coefficients are similar for the cases of Poiseuille flow and plug flow, but the difference between these two dispersion coefficients is larger for a thin annulus. For the case of large interfacial mass-transfer resistance, the average equations cannot be expressed as the con-

vection–diffusion equation. The results of this study are of relevance to dispersion in tissues, where the mechanisms proposed in this paper can augment the dispersion of solutes. The calculated values of dispersion coefficients for certain tissues are of the same order of magnitude as the experimentally determined values. This suggests that the proposed mechanism for dispersion is relevant to solute transport in capillaries.

Acknowledgments

The authors acknowledge the financial support of the Engineering Research Center (ERC) for Particle Science and Technology at the University of Florida, The National Science Foundation (NSF Grant EEC-94-02989), and the Industrial Partners of the ERC for support of this research. Any opinions, findings, and conclusions or recommendations expressed in this material are those of the authors and do not necessarily reflect those of the National Science Foundation.

Notation

a = parameter that describes the radius of the combined tube and surrounding annulus
Bi = Biot number, dimensionless mass-transfer coefficient, $\kappa R/D$
$\widetilde{\text{Bi}}$ = scaled Biot number, $\kappa L/D$
C = total solute concentration in the tube
C^* = reference drug concentration
C_t = solute concentration in the annulus
$\tilde{C}$ = dimensionless solute concentration in the tube
$\tilde{C}_t$ = dimensionless solute concentration inside the annulus
D = solute diffusion coefficient in the tube
D^* = dispersion coefficient in the tube
D_t = diffusion coefficient within the annulus
D_N = Oliver et al.'s dispersion number for a specific tissue
D_N^* = calculated dispersion number for a specific tissue used for comparison with Oliver et al.'s dispersion number
$\tilde{D}^*$ = dimensionless dispersion coefficient
$\tilde{D}_0^*$ = contribution of the effective molecular diffusivity to dispersion
$\tilde{D}_{po}^*$ = dimensionless dispersion coefficient for Poiseuille flow
$\tilde{D}_{pl}^*$ = dimensionless dispersion coefficient for plug flow
$\tilde{D}_c^*$ = part of the contribution of convection to dispersion (dimensionless)
$\tilde{D}_{c\,po}^*$ = convective contribution to dispersion for Poiseuille flow (dimensionless)
$\tilde{D}_{c\,pl}^*$ = convective contribution to dispersion for plug flow (dimensionless)
$\tilde{D}_R^*$ = contributions of the interfacial resistance to mass transfer to dispersion (dimensionless)
K = solute's tube:annulus partition coefficient
L = length of the tube
n_c/A = capillary number density
Pe = Peclet number, $\langle u\rangle R/D$
r = radial coordinate
$\tilde{r}$ = dimensionless radial coordinate
Q = flow rate of blood leaving the tissue
R = radius of the tube
t = time
$\tilde{t}$ = dimensionless time
$\tilde{t}_x$ = dimensionless timescale for transport across the capillary wall
$\tilde{t}_l$ = dimensionless timescale for axial diffusion
u_z = velocity of fluid in the tube in the z-direction
$\bar{u}$ = mean velocity of a pulse of solute in the tube
$\tilde{\bar{u}}$ = dimensionless mean velocity of a pulse of solute in the tube
$\langle u\rangle$ = average velocity of fluid in the tube
$\tilde{u}_z$ = dimensionless velocity of fluid in the z-direction
S_c/V = capillary surface area to tissue volume ratio
V = volume of the tissue
z = axial coordinate
z^* = axial coordinate in the moving reference frame
$\tilde{z}^*$ = dimensionless axial coordinate in the moving reference frame

Greek letters

ε = small dimensionless perturbation parameter, R/L
κ = mass-transfer resistance to solute transport at the tube–annulus interface
τ_1 = timescale for transfer of solute from the tube to the annulus at the front end of the parabaloid
τ_2 = timescale for transfer of solute from the annulus to the tube at the back end of the parabaloid
τ_3 = timescale for radial diffusion within the tube
τ_4 = timescale for radial diffusion within the annulus

Literature Cited

1. Taylor GI. Dispersion of soluble matter in solvent flowing slowly through a tube. *Proc R Soc Lond Ser A Math Phys Eng Sci*. 1953;219:186-203.
2. Ananthkrishnan V, Gill WN, Barduhn AJ. Laminar dispersion in capillaries: Part I. Mathematical analysis. *AIChE J*. 1965;11:1063-1072.
3. Gill WN, Sankaras R. Exact analysis of unsteady convective diffusion. *Proc R Soc Lond Ser A Math Phys Eng Sci*. 1970;316:341-350.
4. Sankarasubramanian R, Gill WN. Unsteady convective diffusion with interphase mass transfer. *Proc R Soc Lond Ser A Math Phys Eng Sci*. 1973;333:115-132.
5. Aris R. On the dispersion of a solute by diffusion, convection and exchange between phases. *Proc R Soc Lond Ser A Math Phys Eng Sci*. 1959;252:538-550.
6. Tepper RS, Lee HL, Lightfoot EN. Transient convective mass transfer in Krogh tissue cylinders. *Ann Biomed Eng*. 1978;6:506-530.
7. Levitt DG. Capillary–tissue exchange kinetics—An analysis of the Krogh cylinder model. *J Theor Biol*. 1972;34:103-124.
8. Fournier RL. *Basic Transport Phenomena in Biomedical Engineering*. Philadelphia, PA: Taylor & Francis; 1999.
9. Krogh A. The number and distribution of capillaries in muscles with calculations of the oxygen pressure head necessary for supplying the tissue. *J Physiol*. 1919;52:409-415.
10. Popel AS, Goldman D, Vadapalli A. Modeling of oxygen diffusion from the blood vessels to intracellular organelles. *Adv Exp Med Biol*. 2003;530:485-495.
11. Charm SE, Kurland GS. *Blood Flow and Microcirculation*. New York, NY: Wiley; 1974.
12. Bloor MI. The flow of blood in the capillaries. *Phys Med Biol*. 1968;13:443-450.
13. Burton AC. *Physiology and Biophysics of the Circulation: An Introductory Text*. Chicago, IL: Year Book Medical Publishers; 1965.
14. Alphin RS, Martens JR, Dennis DM. Frequency-dependent effects of propofol on atrioventricular nodal conduction in guinea pig isolated heart. Mechanism and potential antidysrhythmic properties. *Anesthesiology*. 1995;83:382-394.
15. Morey TE, Martynyuk AE, Napolitano CA, Raatikainen MJ, Guyton TS, Dennis DM. Ionic basis of the differential effects of intravenous anesthetics on erythromycin-induced prolongation of ventricular repolarization in the guinea pig heart. *Anesthesiology*. 1997;87:1172-1181.
16. Napolitano CA, Raatikainen MJ, Martens JR, Dennis DM. Effects of intravenous anesthetics on atrial wavelength and atrioventricular nodal conduction in guinea pig heart. Potential antidysrhythmic properties and clinical implications. *Anesthesiology*. 1996;85:393-402.
17. Novalija E, Fujita S, Kampine JP, Stowe DF. Sevoflurane mimics ischemic preconditioning effects on coronary flow and nitric oxide release in isolated hearts. *Anesthesiology*. 1999;91:701-712.
18. Oliver RE, Jones AF, Rowland MA. Whole-body physiologically based pharmacokinetic model incorporating dispersion concepts: Short and long time characteristics. *J Pharmacokinet Pharmacodyn*. 2001;28:27-55.
19. Guyton AC. *Textbook of Medical Physiology*. 7th Edition. Philadelphia, PA: Saunders; 1986.
20. Stroh M, Zipfel WR, Williams RM, Webb WW, Saltzman WM. Diffusion of nerve growth factor in rat striatum as determined by multiphoton microscopy. *Biophys J*. 2003;85:581-588.
21. Altman PL, Katz DD, Grebe RM. *Handbook of Circulation*. Philadelphia, PA: Saunders; 1959.

Manuscript received Aug. 12, 2004, and revision received Jan. 12, 2005.